X-ray investigations of a nematic compound exhibits smectic B phase

S.Mohyeddine, R.Somashekar, D.Revannasiddaiah*

Department of Studies in Physics, University of Mysore, Manasagangotri, Mysore-570 006, (INDIA)
E-mail: dr@physics.uni-mysore.ac.in
Received: 13th May, 2008 ; Accepted: 18th May, 2008

ABSTRACT

Wide angle X-ray patterns were recorded at different temperatures in the nematic and smectic-B phases of 4-hexyl-4′-[2-(4-isothiocyanatophenyl) ethyl]-1,1′-biphenyl. Layer thickness, inter planer spacing and hence the thermal expansion coefficient were determined in smectic-B phase at various temperatures. The orientational distribution function f(β) has been calculated from the angular distribution of the X-ray intensities. The orientational order parameter <P_2>has been determined from f(β). Further, following Line Profile Analysis (LPA), it is examined the X-ray profiles of outer and inner rings to compute the crystallite size and intrinsic strain present in the sample. It has been observed that the crystallite area in the smectic-B phase is larger than that of crystalline phase, which essentially indicates a reordering of molecules with a stronger inter/ intra molecular interaction in smectic-B phase. In addition, it is also observed that nano-crystallite area in SmB phase decreases with increase in temperature.
© 2008 Trade Science Inc. - INDIA

1. INTRODUCTION

Interest in the properties of hexatic smectic B (SmB) phase has been greatly stimulated by recent theoretical and experimental developments[1]. Since the smectic phases have extremely weak interlayer coupling and a variety of two-dimensional (2D) intralayer structures, they are reasonably good models for the study of weakly interacting 2D systems[1]. The layered SmB liquid crystalline phase is the only two dimensional physical system in which hexatic orders are observed[2,3]. This ordering involves a long-range six-fold symmetric, orientational alignment of the bond connecting neighbouring in-plane molecules even though their in-plane positional correlations remain short ranged[4, 5]. The orientational

distribution function f(β) relative to the director of a nematic liquid crystal can be determined by exploiting the X-ray wide angle diffuse ring corresponding to the lateral mean distance between nearest neighbour molecules[6]. Here we have investigated smectic B and nematic phases of 4-hexyl-4′-[2-(4-isothiocyanato phenyl) ethyl]-1,1′-biphenyl (HIEB) using X-ray technique.

2. EXPERIMENTAL

The sample studied here was obtained from M/s Aldrich Chemical Company Inc. (USA). The crystal to SmB, SmB to nematic and nematic to isotropic transition temperatures were determined using the polarizing microscope and a specially constructed hot stage. The

Figure 1: A typical SmB phase texture photograph observed between crossed polarizers (homeotropic alignment)
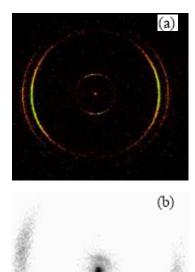

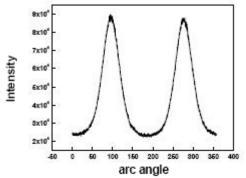**Figure 2: X-ray diffraction patterns of HIEB (a) SmB and (b) Nematic**

Figure 3: X-ray Intensity profile as a function of arc angle in the nematic phase

values are found to be respectively 60.3, 98.5 and 130.8°C. A typical SmB phase texture photograph observed between crossed polarizers is shown in figure 1. X-ray diffraction recordings were carried out using

CuKα radiation (λ = 1.5418Å) from a fine focus sealed-tube generator in conjunction with double mirror focusing optics.

The mirror optics provides a nearly parallel beam over a long working distance. In recording the X-ray intensity data, the sample was taken in a capillary tube. The detector was an image plate detector (MAC Science, Japan, model DIP 1030) with an effective resolution of 100×100 μm^2. The temperature of the sample was controlled with the help of a hot stage, of Mettler Toledo (model FP 82/HT). Representative X-ray patterns recorded in SmB and nematic phases are shown in figure 2. Using the supplied X-ray software, circular scan of diffused ring was performed to obtain intensity versus arc angle. Such intensity data were obtained at various temperatures in the nematic phase of the sample in steps of 5°C. Figure 3 shows the representative X-ray arc intensity profile recorded in nematic phase at 110°C Other details of experimental techniques have already been discussed elsewhere[7].

3. THEORY

3.1. Calculation of the distribution function and microscopic order parameter using X-ray data

Liquid crystalline phases are characterized by the existence of long or quasi-long-range orientational order for their elongated, rod-like molecules[8]. This is, in fact, the main feature of nematic phase distinguishing them from isotropic liquids. The orientational order parameter is essentially the second moment of orientational distribution function f(β). Falgueirettes (1955)[9], Delord and Falgueirettes (1965)[10], de Varies (1972)[11] and Leadbetter et al.[6, 12, 13] have discussed methods of computing the nematic orientational order parameter from X-ray arc intensity data. The simplest approach is that of Leadbetter, and it was widely applied to many mesogenic compounds[14-18] which lead to a classical formula.

$$I(\phi) = \int_{0}^{\pi/2} f(\beta)\sec^2(\phi)\,(\tan^2\beta - \tan^2\phi)^{-1/2}\sin(\beta)d\beta \qquad (1)$$

where, β is the angle between the rod axis and the director. The integral equation is usually numerically inverted by assuming, in most cases, a more or less specific expansion of I(φ) and $f(\beta)$. To evaluate the orientational distribution function f(β)

Full Paper

and the order parameters, various numerical and series expansion methods have been employed[16-19]. Deutsch[20] has derived an exact analytical solution to Eqn. (1) and has obtained the expression for the order parameter <P$_2$> and higher order parameter <P$_4$>as:

$$\langle P_2 \rangle = 1 - \frac{3}{2N}$$
$$\int_0^{\pi/2} I(\phi)\left[\sin^2\phi + \sin\phi\cos\phi\log\left(\frac{1+\sin\phi}{\cos\phi}\right)\right]d\phi \tag{2}$$

and

$$\langle P_4 \rangle = 1 - \frac{1}{N}$$
$$\int_0^{\pi/2} I(\phi)\,[\sin^2\phi\,(\frac{105}{16}\cos^2\phi + \tag{3}$$

$$(\sin\phi)\log(\frac{1+\sin\phi}{\cos\phi})(\frac{105}{16}\cos^4\phi - \frac{15}{4}\cos^2\phi)]\,d\phi$$

Where, $N = \int_0^{\pi/2} I(\phi)\,d(\phi)$

The Leadbetter expression for $I(\phi)$ in terms of a series can be written as:

$$I(\phi) = f_0 + \frac{2}{3}f_2\cos^2\phi + \frac{8}{15}f_4\cos^4\phi + \frac{16}{35}f_6\cos^6\phi +$$
$$\frac{128}{315}f_8\cos^8\phi + \frac{256}{693}f_{10}\cos^{10}\phi + ... \tag{4}$$

Within the framework of Maier-Saupe model, Levelut group[21] have come up with a novel method wherein there is only one independent parameter 'm' to compute orientational order from arc intensity $I(\phi)$ and the expression is:

$$I(\phi) = i/Z\,[1 + (2m/3)\cos^2\phi + (4m^2/15)\cos^4\phi +$$
$$(8m^3/105)\cos^6\phi + (16m^4/945)\cos^8\phi + ...] \tag{5}$$

Where $Z = 4\pi\int_0^1 e^{mx^2}dx$ is the normalization constant. The constant f in Leadbetter approach and the constant m in Levelut method are related to the order parameter via the orientational distribution function[21] as:

$$<\cos^2\beta> = J_2(m)/J_0(m) \tag{6}$$

and

$$<\cos^2\beta> = J_2(m)/J_0(m) \tag{7}$$

The relation involving f is given by

$$<\cos^2\beta> = \frac{\sum_{i=0}^{\infty} f_{2i}/(2i+3)}{\sum_{i=0}^{\infty} f_{2i}/(2i+1)} \tag{8}$$

The orientational distribution function f(β)has been calculated from the angular distribution of the X-ray intensities. The orientational order parameter <P$_2$> has been determined from f(β). We have written suitable FORTRAN programmes to estimate the order parameters <P$_2$> from the different approaches described above.

3.2. Line profile analysis: Estimation of nano-crystallite area in SmB phase

Diffraction technique is used to obtain nano-structural information of the sample averaged over the diffraction volume.

Warren and Averbach method [1959,1960], which is based on the imperfections of the structure (e.g. crystallites size and lattice strain) cause broadening of the diffraction line profiles[22,23]. For this purpose, we have used Bragg reflections observed in SmB phase. The Intensity profile can be expanded using Fourier Cosine series[23,24] and is given by:

$$I(s) = \sum_{n=\infty}^{-\infty} A(n)\cos\{2\pi nd(s-s_o)\} \tag{6}$$

where, A(n) are the coefficients of harmonics and can be represented as a function of crystal size and lattice distortion (g, strain), d is the interplanar spacing , s is the value of $\{\sin(\theta)/\lambda\}$, s$_o$ is the value of s at peak of the reflection, θ is the Bragg's angle, λ is the wavelength of the radiation and n is the harmonic number. The Fourier coefficients A(n) of the profile are expressed as the convolution of crystallite size A$_s$(n) and lattice strain coefficients A$_d$(n):

$$A(n) = A_S(n).A_d(n) \tag{7}$$

with D=N.d$_{hkl}$. In case of a liquid crystal (e.g. SmB) it is rare to find multiple reflections and hence we cannot use Warren and Averbach multiple order method. We have used single order method to estimate nano-crystallite area and lattice strain, using an exponential function[25-27] for P(i). This distribution depends on the fact that there are no columns containing fewer than p number of unit cell and those with more than p will decay exponentially where the width of the distribution is α=1/(N-p). Hence P(i) can be expressed as :

$$P(i) = \begin{cases} 0 & \text{if} \quad p<i \\ \alpha \exp\{-\alpha(n-p)\} & \text{if} \quad p\geq i \end{cases} \qquad (8)$$

after substituting in Eq (8) and further simplifying, we have:

$$A_S(n) = \begin{cases} A(0)\left(1-\dfrac{n}{N}\right) & \text{if} \quad n\leq p \\ A(0)\exp\{-\alpha(n-p)\}/(\alpha N) & \text{if} \quad n>p \end{cases} \qquad (9)$$

The experimental profiles between s_o (the scattering vector at the peak) and $S_o + S_o/2$ is matched with the simulated profiles obtained using Eqs. (6-11) for various values of $<N>$, g, α and background correction (BG). For this purpose we have used a multidimensional minimization program SIMPLEX[28]. The goodness of the fit between experimental and simulated intensity profiles, has been computed by the relation:

$$\Delta^2 = [I_{cal} - (I_{exp} + BG)]^2 \,/\, \text{number of points} \qquad (12)$$

Here I_{cal}, I_{exp} and BG represent the calculated intensity, experimental intensity and background correction of the profile. We have used two reflections, wherein one is at lower angle (2.90-2.88°) and another one at larger angle (19.35-19.56°) to compute micro-structural parameters in SmB phase. The ones at the larger angle are due to the interaction of neighbouring, parallel molecules and the average distance between the long axes of the molecules (inter planer spacing d). The maxima at the smaller diffraction angle are related to the length of the molecule or the layer thickness l[29,30]. For a better perspective, we have projected the parameters in two dimensions using the relation[31]:

$$(2/D_{hkl}^2) = (\cos\varphi/Y)^2 + (\sin\varphi/X)^2 \qquad (13)$$

where, φ is the angle between the planes giving the Bragg reflections. The best values of Y and X are obtained based on iterative procedure.

4. RESULTS AND DISCUSSION

The variation of the distribution function f(β) with temperature in the case of HIEB is shown in figure 4. It can be noted from the figure that the distribution function f(β)is more fundamental than the order parameter. The orientational order parameter $<P_2>$ is directly related to the measure of variance (width) of f(β). The higher order parameter $<P_4>$, which is a measure of peakedness of f(β). It is evident from figure 4 that, with
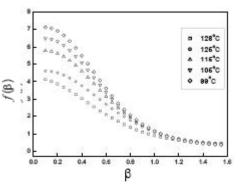

Figure 4: The distribution function as a function of β in nematic phase
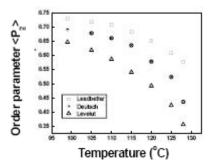

Figure 5: Order parameter as a function of temperature

increase in temperature $<P_2>$as well as $<P_4>$ decrease showing that there is a decrease in the ordering of the molecules in the nematic phase. The values of $<P_2>$ so estimated are shown graphically in figure 5. It is evident from figure 5 that the trend in the variation of $<P_2>$ computed from the different methods is the same. However, the values computed from the Deutsch method lies in between the values computed by the Leadbetter et al. and Levelut methods. Deutsch is more reliable because of the fact that it involves the computations of the orientational order parameter using analytically obtained solutions. The discrepancy in Leadbetter and Levelut methods are due to the truncation of the series to a finite number of terms, whereas the solution is exact in Deutsch method. Figure 6(a, b) shows two intensity profiles of Bragg reflection at 75°C in SmB phase, one at angle $2\theta = 2.90^0$ (inner) and the other at $2\theta = 19.49^0$ (outer). The values of the apparent molecular length or layer thickness l and the intermolecular distance or the inter planer spacing d at different temperatures are also measured. The temperature variation of the layer thickness and intermolecular spacing are shown in figure 7. There is an increase in the inter planer spacing with the increase in temperature. From
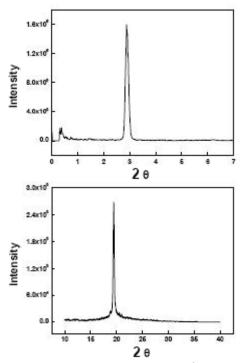
Full Paper

Figure 6: X-ray Intensity profiles at 75⁰C in SmB phase. (a) at smaller angle (inner) scan and (b) at larger angle (outer) scan
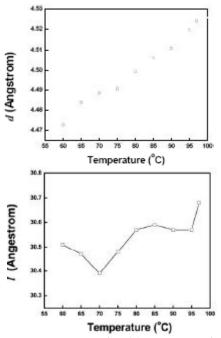

Figure 7: Inter planer spacing (a) and layer thickness (b) versus temperature in SmB phase

the measured inter planer spacing the thermal expansion coefficient was found to be $\{\alpha = 1.3 \times 10^{-3}\ (\text{Å}/^{\circ}C)\}$. This indicates the possible stretching of smectic layers within the SmB phase. The results of line profile analysis are

TABLE 1(a): The micro-structural parameters at different temperatures in the SmB phase determined using line analysis profile, at higher angle

Sample	2θ (degree)	d_{hkl} (Å)	N	g (%)	D_s (Å)	Delta
60	19.58	4.59	54.23	0.1	248.92	0.057
65	19.54	4.54	57.24	0.1	259.87	0.045
70	19.50	4.55	54.74	0.1	249.07	0.063
75	19.49	4.55	53.94	0.1	245.43	0.063
80	19.47	4.56	56.32	0.1	256.82	0.060
85	19.45	4.56	54.33	0.1	247.74	0.059
90	19.40	4.57	55.83	0.1	255.14	0.058
95	19.35	4.58	55.31	0.1	253.32	0.058
97	19.39	4.58	54.20	0.1	248.24	0.057

TABLE 1 (b): The micro-structural parameters at different temperatures in the SmB phase determined using line analysis profile, at lower angle

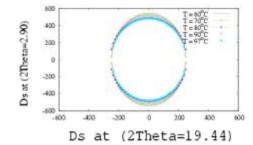| Sample	2θ (degree)	l (Å)	N	g (%)	D_s (Å)	delta
60	2.90	30.51	17.81	0.1	543.31	0.0612
65	2.90	30.47	17.70	0.1	539.40	0.0624
70	2.91	30.39	17.30	0.1	525.76	0.0550
75	2.90	30.48	17.41	0.1	530.70	0.0576
80	2.89	30.57	16.02	0.1	489.74	0.0580
85	2.89	30.59	18.45	0.1	564.33	0.0564
90	2.89	30.57	16.47	0.1	503.49	0.0583
95	2.89	30.57	15.22	0.1	465.28	0.0593
97	2.88	30.68	15.70	0.1	481.62	0.0563

Figure 8: Variation of nano-crystallite area with temperature in SmB Phase

given in TABLE 1(a,b). It is evident from this TABLE that the intrinsic strain in SmB phase is almost negligible at all temperatures. Further, we also observe that the nano-crystallite area in SmB phase at any temperature is much greater than that in the crystalline phase. This indicates that ordering exists over a large area of smectic layers due to pair-wise interactions. Secondly the nano-crystallite area decreases with increase in temperature in SmB phase (see, figure 8) and is in agreement with the understanding of the fact that the smectic layers and their ordering are affected by the thermal energy.

Full Paper

5. CONCLUSIONS

In this paper, we have recorded X-ray diffraction patterns in nematic and SmB phases of HIEB. Based on the computed orientational order parameter by different theoretical approaches it is found that the Deutsch method is more reliable than that of the other methods. From the computed nano-crystallite area in SmB phase it is observed that the nano-crystallite area in SmB phase is greater than that of the crystalline phase.

6. ACKNOWLEDGMENTS

7. REFERENCES

[1] C.Jeffrey, L.B.Sorensen, P.S.Pershan; Phys.Rev., **32**, 1036 **(1985)**.

[2] R.Pindak, D.R.Moncton, S.C.Davey, J.W.Goodby; Phys.Rev.Lett., **46**, 1135 **(1981)**.

[3] S.C.Davey, J.Pudai, J.W.Goodby, R.Pindak; Phys. Rev.Lett., **53**, 2129 **(1984)**.

[4] R.Bruinsma, G.Aeppli; Phys.Rev.Lett., **48**, 1625 **(1982)**.

[5] V.L.Chethan, S.K.Prasad, D.S.Shankar Rao; Phys. Rev., **69**, 57106 **(2004)**.

[6] A.J.Leadbetter, E.K.Norris; Mol.Phys., **38**, 669 **(1979)**.

[7] V.L.Chethan, S.K.Prasad, D.S.Shankar Rao; Phys. Rev., **72**, 062701 **(2005)**.

[8] P.S.Pershan; 'Structure of Liquid Crystal Phases', World Scientific, Singapore, **(1988)**.

[9] J.Falgueirettes; Bull.Soc.France, **82**, 171 **(1959)**.

[10] P.Delord, J.Falgueirettes, C.R.Acad; Sci.Paris, **260**, 2468 **(1965)**.

[11] A.de Vries; J.Chem.Phys., **56**, 4489 **(1972)**.

[12] A.J.Leadbetter, G.Lukhurst, G.W.Gray; 'The Molecular Physics of Liquid Crystals', Academic Press, New York, **(1979)**.

[13] A.J.Leadbetter, P.G.Wrighton; J.Phys.Colloq. France, **40**, C3-324 **(1979)**.

[14] W.Haase, Z.X.Fan, H.G.J.Muller; J.Chem.Phys., **89**, 3317 **(1988)**.

[15] B.Bhattacharjee, S.Paul, R.Paul Mol.Cryst.Liq. Cryst., **44**, 1391 **(1981)**.

[16] Buman, Z.X.Fan, W.Haase; Liq.Cryst., **6**, 239 **(1989)**.

[17] Z.X.Fan, S.Buchner, W.Haase, H.G.Zachmann; J. Chem.Phys., **92**, 5099 **(1990)**.

[18] D.Gopalakrishna, D.Revannasiddaiah, R. Somashekar; Mol.Cryst.Liq.Cryst., **437**, 121 **(2005)**.

[19] V.K.Kelkaz, A.S.Paranjape; Mol.Cryst.Liq.Cryst. Lett., **4**, 1391 **(1987)**.

[20] M.Deutsch; Phys.Rev., **44**, 8264 **(1991)**.

[21] P.Davidson, D.Petermann, A.M.Levelut; J.Phys.II, **5**, 113 **(1995)**.

[22] B.E.Warren, B.L.Averbach; J.Appl.Phys., **23**, 497 **(1952)**.

[23] B.E.Warren; Acta Cryst., **8**, 483 **(1955)**.

[24] R.Hosemann; Colloid Polym.Sci., **260**, 864 **(1982)**.

[25] N.C.Pope, D.Balzar; J.Appl.Cryst., **35**, 338 **(2002)**.

[26] D.Balzar; Appl.Crystallog., **37**, 911 **(2004)**.

[27] I.H.Hall, R.Somashekar; J.Appl.Cryst., **24**, 1051 **(1991)**.

[28] W.Press, B.P.Flannery, S.Teukolsky, W.T.Vetterling; 'Numerical Recipe', Cambridge University Press, **(1986)**.

[29] A.de Vries; Mol.Cryst, Liq.Cryst., **10**, 219 **(1970)**.

[30] M.K.Das, P.D.Roy, S.Paul, R.Paul, B.Das; Mol. Cryst.Liq.Cryst., **55**, 457 **(2006)**.

[31] H.Somashekarappa, R.Somashekar, Vasudev Singh, S.Z.Ali; Bull.Mater.Sci., **22**, 101 **(1999)**.